PAPER • OPEN ACCESS

Thermodynamics performance optimization of a hybrid solar gas turbine power plant in Colombia

To cite this article: F Moreno-Gamboa *et al* 2022 *J. Phys.: Conf. Ser.* **2163** 012004

View the article online for updates and enhancements.

Thermodynamics performance optimization of a hybrid solar gas turbine power plant in Colombia

F Moreno-Gamboa[1]**, J C Acevedo-Paez**[2]**, and D Sanin-Villa**[3]

[1] Grupo de Investigación en Fluidos y Térmicas, Universidad Francisco de Paula Santander, San José de Cúcuta, Colombia

[2] Grupo de Investigación Eureka, Universidad de Santander, San José de Cúcuta, Colombia

[3] Grupo de Investigación en Automática, Electrónica y Ciencias Computacionales, Instituto Técnico Metropolitano, Medellín, Colombia

E-mail: faustinomoreno@ufps.edu.co

Abstract. A thermodynamic model is presented for evaluation of a solar hybrid gas-turbine power plant. The model uses variable ambient temperature and estimates direct solar radiation at different day times. The plant is evaluated in Barranquilla, Colombia, with a solar concentration system and a combustion chamber that burns natural gas. The hybrid system enables to maintain almost constant the power output throughout day. The model allows optimizing the different plant parameters and evaluating maximum performance point. This work presents pressure ratio ranges where the maximum values of overall efficiency, power output, thermal engine efficiency and fuel conversion rate are found. The study is based on the environmental conditions of Barranquilla, Colombia. The results obtained shows that optimum pressure ratio range for power output and overall efficiency is between 6.4 and 8.3, when direct solar radiation its maximum at noon. This thermodynamic analysis is necessary to design new generations of solar thermal power plants.

1. Introduction

Solar concentration systems coupled to thermal generation plants are presented as a total or partial source of heat supply to power cycles [1]. Within these concentration systems, there are several technologies under development, where heliostat field systems and central tower with receiver stand out, due to the wide range of concentration ratios that can be managed with this technology [2]. At present, there is great interest in use of heliostat and tower systems as an energy source for gas turbines, given their great flexibility in configurations and power ranges [3]. These systems can be operated at high temperatures with low water availability in areas with high solar radiation values [4].

Some studies have focused on the optimization of heliostat fields, which depend drastically on their location [5], others in the configuration and operation of the central receiver, whose optimal characteristics remain an open work area [6]. However, our focus is on a simple model for the whole plant, which includes the main irreversibility of system. Additionally, the use of a solar resource estimation model is proposed as a complementary source of energy for gas turbine and a combustion chamber to complete hybridization of system [7].

The Solugas experimental plant in Seville, Spain, is the only heliostat field plant and central tower operating with 4.6 MW gas turbine [8]. In the northern of Colombia is viable the use of solar resource

for the operation of solar concentration systems [9]. This paper presents the evaluation of a hybrid Brayton cycle solar plant in Barranquilla, Colombia. The design parameters of the Solugas experimental plant are used in the simulation. Finally, the optimal values of different operating parameters of plant are estimated, based on overall pressure ratio, especially power, overall efficiency, thermal engine efficiency and fuel conversion rate.

2. Solar hybrid thermal power plant and models
This section presents hybrid solar gas turbine scheme, direct solar radiation estimation model and thermodynamic model of system.

2.1. Overall plant model
Evaluation of the hybrid solar gas-turbine is developed from the scheme presented in Figure 1; the components of power plant are shown in Figure 1(a). Figure 1(b) presents the entropy temperature diagram with the heat fluxes. The working fluid develops a closed Brayton cycle, first process is a compressor (1-2). The heat sources are the regenerator (2-x), the solar receiver (x-y) and combustion chamber (y-%); below is the turbine (3-4). Finally, the plant dissipates heat to the environment through a heat exchanger (z-1); the working fluid was considered air.
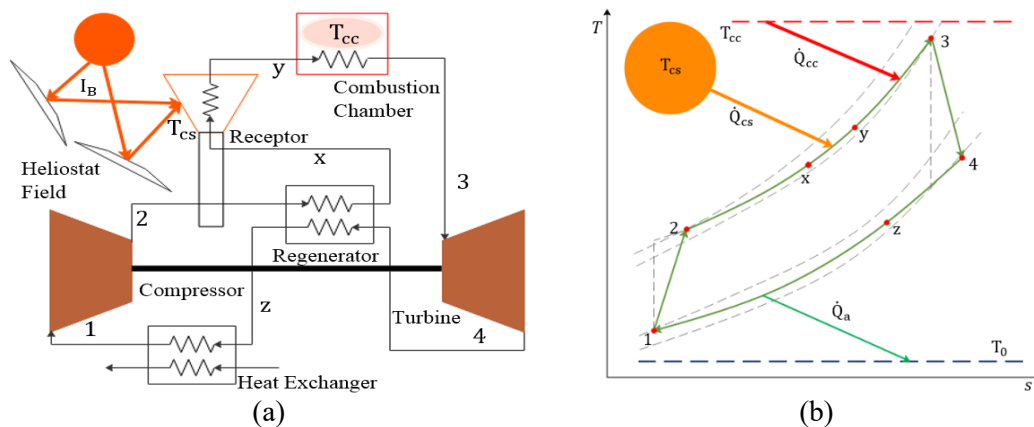

Figure 1. (a) Scheme of solar hybrid gas-turbine plant; (b) temperature vs entropy diagram.

2.2. Solar model
The operation of the system needs direct solar radiation values, these values are estimated with the daily integration approach model (DI model) [10]; in DI model the solar direct radiation (I_B) is defined in Equation (1) [10].

$$I_B = r_t \, \overline{H}_H - r_d \, \overline{D}_H, \tag{1}$$

where r_d is the hour to day relationships for diffuse radiation, and r_t is the hour to day relationships for diffuse global radiation, $\overline{H}_h$ and $\overline{D}_h$ represent the long-term monthly daily average for total and diffuse radiation, the values are available from the National Aeronautics and Space Administration (NASA) prediction of energy resources website [11].

2.3. Power unit model
Following the work of Moreno-Gamboa, *et al*. [12], the values of $\dot{Q}_{cs}$ and $\dot{Q}_{cc}$ represent the external heat delivered to the working fluid by the solar concentrating system and the combustion chamber respectively (see Figure 1(b)). Therefore, $\dot{Q}_H$ is defined as the total heat supplied to the working fluid and is expressed in Equation (2). In the evaluation of different parameters of cycle, (h) represents the enthalpy of each state and (ṁ) is mass flow rate of the working substance.

$$\dot{Q}_H = \dot{Q}_{cc} + \dot{Q}_{cs} = \dot{m}(h_3 - h_y) + \dot{m}(h_y - h_x) = \dot{m}\,(h_3 - h_x). \tag{2}$$

The solar fraction (f) is the ratio of the solar heat rate that the working fluid absorbs ($\dot{Q}_{cs}$) with respect to the total heat input ($\dot{Q}_H$) and as defined in Equation (3).

$$f = \dot{Q}_{cs}/\dot{Q}_H = \dot{Q}_{cs}/(\dot{Q}_{cc} + \dot{Q}_{cs}). \tag{3}$$

The power output of the solar thermal hybrid plant ($\dot{W}$) is evaluated with Equation (4).

$$\dot{W} = \dot{m}(h_3 - h_4) + \dot{m}(h_2 - h_1) = \dot{Q}_H - \dot{Q}_a, \tag{4}$$

where $\dot{Q}_a$ is the heat dissipated in the heat exchanger with the environment, Equation (5).

$$\dot{Q}_a = \dot{m}(h_z - h_1). \tag{5}$$

The global energy efficiency (η_g) of hybrid solar Brayton cycle is represented in Equation (6), where Q_{lhv} is the lower heating value of the fuel, $\dot{m}_f$ is the fuel mass flow rate, and A_o is the solar receptor area.

$$\eta_g = \dot{W}/(\dot{m}_f \cdot Q_{lhv} + I_B \cdot A_o). \tag{6}$$

The thermal engine efficiency (η_b), is the fraction between the net power output and the total heat input received by the working fluid. η_b is defined in Equation (7).

$$\eta_b = \dot{W}/\dot{Q}_H. \tag{7}$$

Fuel consumption ($\dot{m}_f$) is a function of Q_{lhv}, the efficiency of the combustion process (η_{cc}), and the effectiveness of combustion chamber heat exchanger (ε_{cc}), Equation (8).

$$\dot{m}_f = \dot{m}(h_3 - h_y)/(Q_{lhv} \cdot \eta_{cc} \cdot \varepsilon_{cc}). \tag{8}$$

The plant's fuel conversion rate (r_f) is the fraction between the net power outputs and energy of fuel consumed and is defined in Equation (9).

$$r_f = \dot{W}/(\dot{m}_f \cdot Q_{lhv}). \tag{9}$$

Finally, the compressor pressure ratio (r_c), and the turbine pressure ratio (r_t) are defined in Equation (10) and Equation (11), respectively.

$$r_c = r_p, \tag{10}$$

$$r_t = Di \cdot Ds \cdot r_p. \tag{11}$$

where, r_p is the global pressure ratio, and Di and Ds are the pressure loss factors [12].

3. Result and discussion
The values obtained with the DI model are compared to those reported by the San Lucar station, Seville, Spain, the mean absolute bias error 0.211085%, and the root mean square error 0.226616%. The DI model implemented achieves results fitted in good agreement with the experimental data [13].

Numerical results reported by Merchán, *et al.* [14] are used to validate the thermodynamic model. The results shows a good agreement with the reference data with an acceptable error level (see Table 1). Details of validation, parameters, and models can be found explained in Moreno-Gamboa, *et al.* [12].

Table 1. Thermodynamic model assessment.

	$\dot{W}$ (kW)	η_b	η_g	f
Estimated model	4615.15	0.385	0.302	0.338
Reference	4647.00 [14]	0.393 [14]	0.300 [14]	0.341 [14]
Deviation %	0.69	2.07	0.66	0.88

Figure 2 represents the daily evolution of power output, $\dot{W}$ present a variation of 3% during a whole day and is independent of solar irradiance and is only function of ambient temperature. In this paper using data of average hourly temperature [15]. Additionally, the global efficiency, is reduced with the solar radiation due to the solar concentration losses, it is observed that $\eta_g = 0.354$ is night average and $\eta_g = 0.30$ at noon. Finally, Figure 2 represents the evolution of solar energy contribution f, the solar factor is maximum at noon and f = 0 at night.
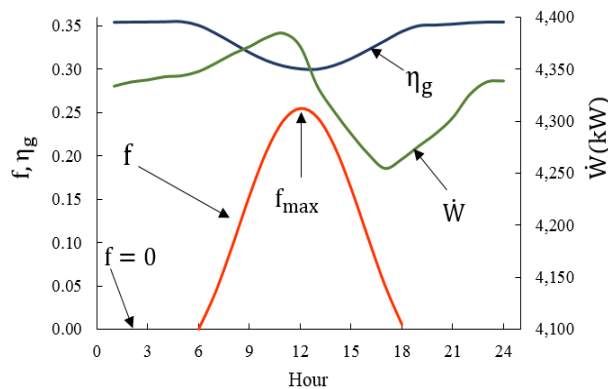

Figure 2. Hourly evolution of overall efficiency and solar fraction.

A typical technique used in gas turbines when performing a thermodynamic optimization is the representation of the power-performance diagrams by means of the parametric elimination of some of the global pressure ratio [3]. It is usual that the power-performance curve with respect to the pressure ratio has the appearance of a loop in which the points of maximum power and maximum efficiency are separated by a certain distance. This interval represents the optimal working region of the gas turbine cycle. This is due to the fact that real systems are usually implicitly optimized to work in a regime that constitutes a compromise between maximum efficiency and maximum power with respect to the fuel consumed.

Figure 3(a) shows the overall efficiency curve eliminating the pressure ratio which can be varied from 3 to 18, considering that the pressure ratio of the reference turbine is 9.9 [16], the yellow arrows indicate increasing values of pressure ratio. The curves are presented for two extreme conditions of the gas turbine, such as the lack of solar radiation at 1 a.m. where (f = 0) and when the solar contribution is maximum (f_{max}), considering that in Figure 3(a) the green box represents ($\eta_{g,max}$) and the blue line ($\dot{W}_{max}$).

In general, it is observed that the maximum efficiency points are at lower pressure ratios between 5.8 and 6.4, while the maximum power points are at pressure ratio values between 8.1 and 8.3, which indicates that the Mercury 50 turbine is designed to operate near its maximum power output [17]. Regarding the influence of solar contribution curves of (f = 0) and (f_{max}), it is observed that the solar

concentration system affects global efficiency, generating a decrease of 16.5% in the maximum value of η_g and allowing said maximum value to reach higher values pressure ratio. The solar concentration system does not show a significant variation in power since it depends more on the maximum temperature of the turbine inlet, which is controlled by the combustion chamber.

Regarding the efficiency of the thermal engine (see Figure 3(b)), a low influence of the solar concentration system is observed since the maximum value of η_b barely varies by 3.6% between pressure ratio values of 4.9 and 5.8. In the thermal engine efficiency, the heat losses in the solar concentration system and the combustion chamber are not considered.
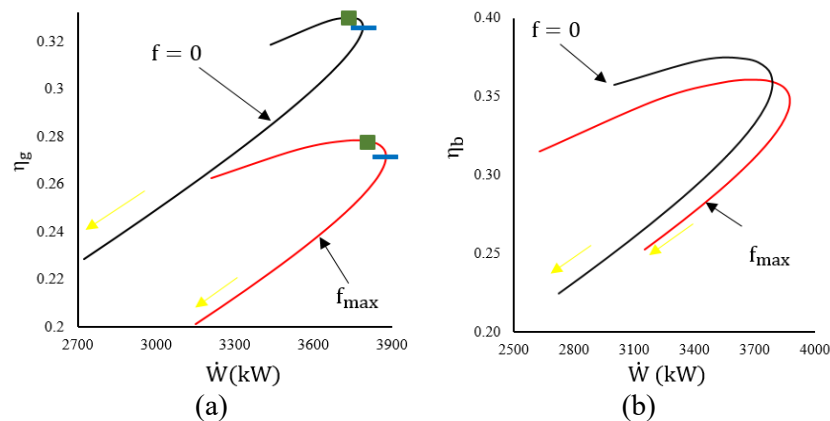

Figure 3. (a) Implicit power output - overall efficiency curves; (b) power output - thermal engine efficiency curves.

The fuel conversion rate is also a function that presents maximum values and is susceptible to optimizing and rationing it with power and efficiency, as observed in Figure 4. In the relationship between r_f and $\dot{W}$, it is observed that the solar concentration system helps to improve the fuel conversion rate significantly, reaching an increase of 42.6% in its maximum value with a pressure ratio range from 4.7 to 5.8.

Additionally, when $f = 0$ the behavior of the r_f vs. $\dot{W}$ curve (see Figure 4(a)) is like the behavior of the curve η_b vs. $\dot{W}$ in Figure 3(a), because $r_f = \eta_g$ when there is no solar resource, as observed in the Equation (6) and Equation (9). This is also reflected in Figure 4(b) when $f = 0$, showing a straight line with the same maximum point.
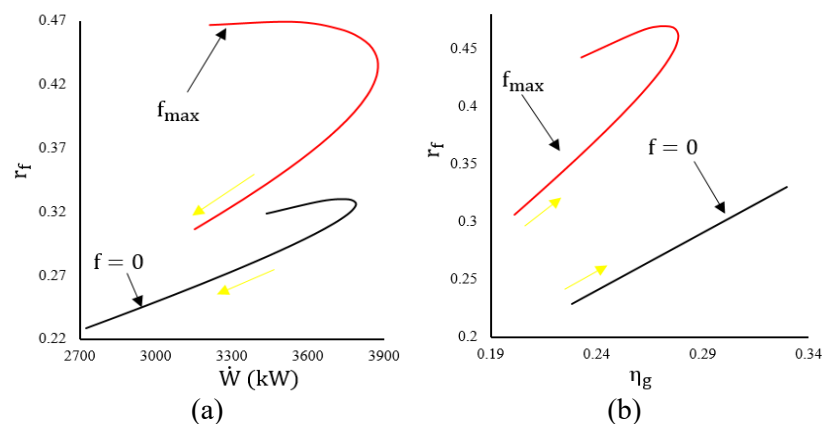

Figure 4. (a) Implicit fuel conversion rate - power output curves; (b) fuel conversion rate - thermal engine efficiency.

Figure 5 shows the relationship between fuel consumption and power (Figure 5(a)) and overall efficiency (Figure 5(b)); there are no maximum values for fuel consumption and if there are maximum values for $\dot{W}$ and η_g therefore fuel consumption grows continuously with increasing pressure ratio although it is not linear.
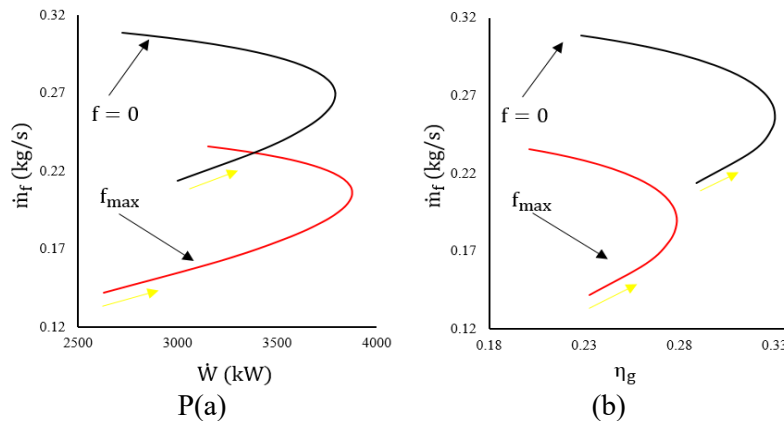

Figure 5. (a) Implicit fuel consumption - power output curves; (b) fuel consumption – overall efficiency.

4. Conclusions

In turbine thermodynamic analyzes, it is typical that the maximum values of power and overall efficiency with respect to the global pressure ratio determine the proper operating range. However, the maximum points are modified by hybridization, due to the variations in the income and the energy demands that occur in the solar concentration system.

Due to the control over the operation that can be performed with the combustion chamber, the power output is not significantly affected, contrary to global efficiency of system. In general, the optimal range of power output-global efficiency curve is established at global pressure ratio values of (6.4 to 8.3) when there is no solar resource and changes to (5.8 to 8.1) when the solar factor is maximum in Barranquilla, Colombia. On the other hand, the fuel conversion factor extends this range up to global pressure ratio values of 4.8. Finally, variables such as fuel consumption show continuous growth and therefore do not have a significant effect on the optimal operating range found. The presented model requires a detailed analysis of optical efficiency, the heliostat field distribution and central tower dimensions.

References

[1]   Nathan G J, Jafarian M, Dally B B, Saw W L, Ashman P J, Hu E, Steinfeld A 2018 Solar thermal hybrids for combustion power plant: A growing opportunity *Progress in Energy and Combustion Science* **64** 4

[2]   Duffie J, Beckman W 2013 *Solar Engineering of Thermal Processes* (New Jersey: John Wiley & Sons)

[3]   Sánchez-Orgaz S, Pedemonte M, Ezzatti P, Curto-Risso P L, Medina A, Calvo-Hernández A 2015 Multi-objective optimization of a multi-step solar-driven Brayton plant *Energy Conversion and Management* **99** 346

[4]   Ho C K, Iverson B D 2014 Review of high-temperature central receiver designs for concentrating solar power *Renewable and Sustainable Energy Reviews* **29** 835

[5]   Behar O 2018 Solar thermal power plants - A review of configurations and performance comparison *Renewable and Sustainable Energy Reviews* **92** 608

[6]   Calise F, d'Accadia M D, Libertini L, Vicidomini M 2018 Thermoeconomic analysis of an integrated solar combined cycle power plant *Energy Conversion and Management* **171** 1038

[7]   Merchán R P, Santos M J, Medina A, Calvo Hernández A 2018 Thermodynamic model of a hybrid Brayton thermosolar plant *Renewable Energy* **128** 473

[8]   Korzynietz R, Brioso J A, del Rio A, Quero M, Gallas M, Uhlig R, Ebert M, Buck R, Teraji D 2016 Solugas - Comprehensive analysis of the solar hybrid Brayton plant *Solar Energy* **135** 578

[9]   Guzman L, Henao A, Vasquez R 2014 Simulation and optimization of a parabolic trough solar power plant in the city of Barranquilla by using system advisor model (SAM) *Energy Procedia* **57** 497

[10]   Gueymard C 2000 Prediction and performance assessment of mean hourly global radiation *Solar Energy* **68(3)** 285

[11]   National Aeronautics and Space Administration (NASA) 2020 *Prediction of Worldwide Energy Resources* (Hampton: Langley Research Center)

[12]   Moreno-Gamboa F, Escudero-Atehortua A, Nieto-Londoño C 2020 Performance evaluation of external fired hybrid solar gas-turbine power plant in Colombia using energy and exergy methods *Thermal Science and Engineering Progress* **20** 100679

[13]   Mejdoul R, Taqi M 2012 The mean hourly global radiation prediction models investigation in two different climate regions in Morocco *International Journal of Renewable Energy Research* **2(4)** 578

[14]   Santos M J, Merchán R P, Medina A, Calvo Hernández A 2016 Seasonal thermodynamic prediction of the performance of a hybrid solar gas-turbine power plant *Energy Conversion and Management* **115** 89

[15]   Ramírez-Cerpa E, Acosta-Coll M, Vélez-Zapata J 2017 Análisis de condiciones climatológicas de precipitaciones de corto plazo en zonas urbanas: caso de estudio Barranquilla, Colombia *Idesia* **35(2)** 87

[16]   Quero M, Korzynietz R, Ebert M, Jiménez A A, del Río A, Brioso J A 2014 Solugas – Operation experience of the first solar hybrid gas turbine system at MW scale *Energy Procedia* **49** 1820

[17]   Olivenza-León D, Medina A, Calvo Hernández A 2015 Thermodynamic modeling of a hybrid solar gas-turbine power plant *Energy Conversion and Management* **93** 435